JOURNAL OF MECHANICAL ENGINEERING AND SCIENCES
ISSN: 2289-4659 e-ISSN: 2231-8380
VOLUME 17, ISSUE 2, 2023, 9453 – 9462
DOI: https://doi.org/10.15282/jmes.17.2.2023.4.0748

RESEARCH ARTICLE

# Magnetohydrodynamics analysis of magnetorheological fluid damper

**T.M. Gurubasavaraju[1]* and M. Muralidhar Singh[2]**

[1] Faculty of Mechanical Engineering, Sree Vidyanikethan Engineering College, Mohan Babu University, 517102, Tirupathi, India
Phone: +91 8762722404
[2] RV Institute of Technology and Management, Bengaluru, 560076, Karnataka, India

**ABSTRACT -** A key feature of magnetorheological fluid is its variability of rheological properties in which upon exposing this fluid, the viscosity of the fluid changes accordingly. Hence this nature can be implemented in various engineering applications. To understand its influence in a magnetorheological (MR) damper, it is essential to study the flow behaviour using computational and numerical methods. The main objective of this work is to estimate the influence of the external magnetic field on the fluid flow velocity inside the damper using magnetohydrodynamic analysis. Finite element analysis, magnetostatic analysis, and magnetohydrodynamic (MHD) analysis have been carried out to investigate the change in the shape of the velocity profile across the flow gap of the monotube MR damper under the various magnitude of magnetic force using the MHD module of ANSYS fluent software. The simulation is conducted by considering laminar, steady-state, and incompressible fluid flow. In finite element analysis, the magnitude of magnetic flux density (MFD) 'B' was evaluated at various direct currents. Later, obtained MFD has been applied perpendicular direction to the flow of MR fluid. The effective length of the fluid exposed to the MFD is taken as 2 mm to 28 mm in an overall flow length of 30 mm. The extracted results have shown that the fluid flow velocity reduces with an increase in the magnetic flux density. It has been observed that 10.42 % reduction in velocity upon increasing the magnetic flux density from 0.25 T to 1 T at 75 kPa pressure. The reason for a reduction in velocity is because of variation in the rheological properties of the fluid under the magnetic field, which is very much essential to produce a good damping effect in the MR damper.

**ARTICLE HISTORY**

| | | |
|---|---|---|
| Received | : | 10th Nov. 2022 |
| Revised | : | 01st Feb. 2023 |
| Accepted | : | 25th May 2023 |
| Published | : | 28th June 2023 |

**KEYWORDS**

*Magnetohydrodynamic*
*Non-newtonian fluid*
*Magneto-rheological damper*
*Magnetostatic*

## 1.0 INTRODUCTION

Practical application of magnetorheological (MR) fluid was first introduced by Rabinow in 1947 [1]. In later years, its application got spread to other applications such as MR damper, clutch, bearings, mounts, beams etc [2], [4]. Important aspect of the damper is damping force generated inside the chamber. The variable damping force is influenced by various factors such as the dimension of MR damper, magnetic flux density, current, velocity etc [5][5]. Upon exposing the MR fluid to external stimuli such as magnetic flux, the velocity of the flow tends to decrease due to the sudden variation of the rheological parameters of the fluid such as viscosity. The investigation on the amount of reduction of velocity and response to the external magnetic field has been discussed only in limited publications. Several researchers have adopted computational fluid dynamics (CFD) and finite element (FE) analysis to estimate the variability behavior of MR damper. It has been identified from the literature that a limited interest has been shown in studying the insight of the flow mechanism under various external stimuli using magnetohydrodynamics (MHD). Gedik et al. [6] presented the CFD analysis of molten metal flow and its pattern under external magnetic field by considering various cases. They have found that the velocity of the fluid reduced significantly with external magnetic field. Case et al. [7] presented CFD analysis along with FE analysis of small-scale MR damper through multi-physics modules of COMSOL. The coupling of FEA and CFD was achieved through modified Bingham plastic model. The approach was focused to find feasibility of utilizing MR damper in a medical orthosis for pathological tremor tempering. Sternberg et al. [8] carried out multi-physics formulation and analysis of higher capacity MR damper under various input parameters. Also, an attempt was made to incorporate an external electromagnetic coil design into the MR damper. They have concluded that the MR damper showed increasing damping force with the applied current intensity. Park et al. [9] analyzed MR fluid-based brake in terms of fluid flow and thermal behavior using magnetostatic FE approach. The dynamic behavior and geometric optimization, material selection, and design consideration of MR brake were discussed in the study. Gurubasavaraju [10] evaluated the damping behavior of double-ended MR damper through a one way coupled approach by considering the Hershel-Bulkley flow model. The credibility of the results was verified with analytical calculations and concluded that the one way coupling of fluid flow and magnetostatic would yield promising results. Zschunke et al. [11] developed an analysis model of the MR fluid regime of a damper using commercial software to estimate its dynamic performance. Gedik et al. [12] conducted a CFD study to explore the flow behavior of the MR fluid passing through two fixed plates, which were subjected to the external magnetic field by adopting the MHD module of ANSYS fluent software. The pressure and velocity distribution were presented. Omidbeygi et al. [13] investigated the influence of external magnetic

***CORRESPONDING AUTHOR | T.M. Gurubasavaraju** | ✉ gbrajtm@gmail.com

field on the hydrodynamic behavior of MR fluid across the flow regime through analytical calculations and numerical methods. They have found that influences of MR effects on flow field were significant and not negligible. Diudea et al. [14] carried out CFD analysis of a hydraulic shock absorber of a vehicle using commercial software by adopting dynamic meshing technique to capture the flow streamlines. Tharehallimata et al. [15] carried out one way coupled CFD-FE analysis of MR damper and optimised the design parameters using metaheuristic optimisation techniques. They have concluded that proposed simulation provided promising characteristics of MR damper for the optimisation problem. Zheng et al. [16] presented the computational procedure of design and analysis of multi-stage piston head MR damper and studied the distribution pattern of the magnetic field across the flow region. They had to apply more electromagnetic coils with relative low currents based on the analysis of pressure drop along the annular gap. Nguyen et al. [17] estimated the dimensional geometric factors of designed MR fluid-based valve through FEA based optimization (geometric) technique to enhance the dynamic characteristic. Goldasz [18] developed a mathematical model for monotube MR damper, which could calculate the character of the single cylinder MR damper with various piston configurations. They have concluded that the proposed approach had capability to capture the key performance parameters. Tharehallimata et al. [19] presented magnetostatic investigation to examine the stimulus of the different materials on the MFD induced in the MR fluid flow region. Ferdaus et al. [20] calculated the influence of various physical features of the piston head and electromagnetic coil on the dynamic performance of the MR device using FE analysis. The results revealed that damper with linear gap and chamfered ends provided better performance. Tu et al. [21] estimated the total MFD developed across the fluid flow region of the MR damper using FEA by considering an axisymmetric model. They have concluded that numerical approach would assist designers to provide better configuration of MR dampers. Wang et al. [22] conducted an experimental investigation on the temperature effect on the torque carrying capacity of the MR brake and presented the CFD based analysis at various temperature loading conditions.

Upon thorough observation of literauter survey, it has been inderified that information related to influence of magnetic field on the hydrodynamics of the fluid flow inside the MR damper. The fundamental flow pattern in the flow gap is discussed seldom in the literature. Also, use of MHD in analysing the MR damper by coupling the FE analysis are minimal in the scientific community. Using FE and MHD analysis, variation in the velocity when exposed to the applied MFD can be investigated. The major focus of the present work is to quantify the resistance to the flow parameters of the MRF when it is exposed to external stimuli (magnetic) fields. Under external stimuli, the magnetisable particles are aligned in the field direction to make a chain-like structure which consequently offers a resistance to the fluid flow. Due to this, fluid velocity tends to reduce proportionally with the amount of magnetic field.

## 2.0 METHODOLOGY

The flow chart of the present work is shown in Figure 1. Initially, FE based analysis has been carried out to compute the magnetic flux induced for different current inputs. Then, the obtained average magnetic flux is used to predict the change in the velocity of MR fluid flowing through the gap.

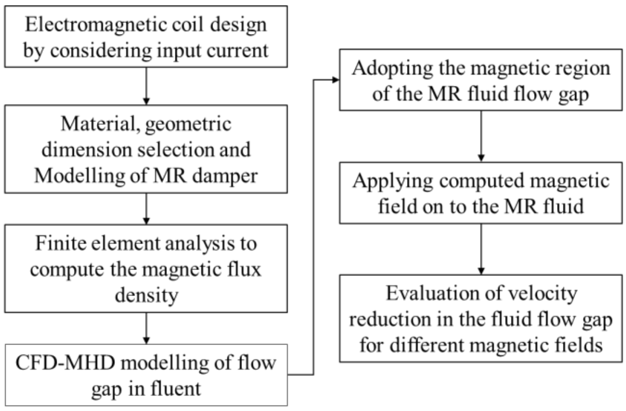


Figure 1. Sequential procedure of methodology

## 3.0 FINITE ELEMENT MODELLING OF MR DAMPER

### 3.1 Electromagnetic Coil Design

The MFD is directly influenced by the number of turns and DC current supplied to the coil. Figure 2 shows the geometrical configuration of the electromagnetic coil fused inside the slot of the piston head. The number of turns in an electromagnetic coil can be calculated by dividing the total area of the rectangular section of the piston where the coil is supposed to wound and by wire cross sectional area which is expressed as:

$$Number\ of\ Turns = \frac{Total\ sectional\ area\ of\ the\ coil}{Cross\ sectional\ area\ of\ the\ wire} = \frac{LB}{\pi d^2/_4} = \frac{22 \times 9}{\pi \times 0.5^2/_4} = 1010$$

where, $d$ is the wire diameter, $L$ is the length of the slot to place wires of the coil and $B$ is the depth of the slot.

The gauge of the copper wire is a very important aspect in the design of electromagnetic coils. The maximum value of current which the copper coil can withstand depends on the gauge of the wire. Here, 20 AWG copper wire is chosen, which is having 0.50 mm diameter and peak value of DC current which can be provided to the wire is 5 A.

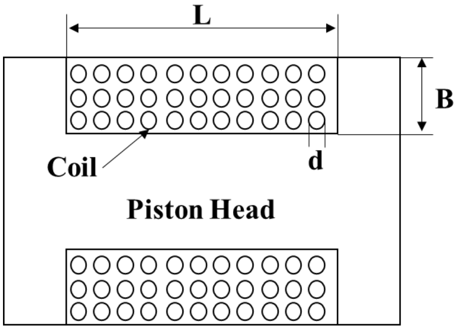


Figure 2. Configuration of piston head and electromagnetic coil

### 3.1 Magnetostatic Analysis

MFD developed across fluid flow area is computed using magneto-static analysis. Typical cross-sectional view and components involved in the MR damper is shown in Figure 3. A section of 2D axisymmetric model, grid model and specification of each components are given in Figure 3(a) and (b), respectively. The MR damper dimensions used are as provided in Table 2 (see Figure 3). The mesh model consists of 6576 triangular elements. While selection of material for each components an important aspect to be keep in mind is that the core part of the piston head should be made of low carbon steel (SA1018) to achieve better magnetic field. The outer cylinder and other parts can be ferrous material but it should be a non-magnetic type. Values of each material properties are accessible in Table 1.

Table 1. Parametric values of each materials of the MR damper components

| Serial No. | Component | Material | Magnetic property |
|---|---|---|---|
| i | Cylindrical tube | 316 Stainless Steel | 1 (Relative permeability) |
| ii | Liquid | MRF-132DG | From B-H curve (Figure 4(a)) |
| iii | Electromagnetic coil | Regular copper | 1 (Relative permeability) |
| iv | Piston Head | Low carbon-SA1018 Steel | From B-H curve (Figure 4(b)) |

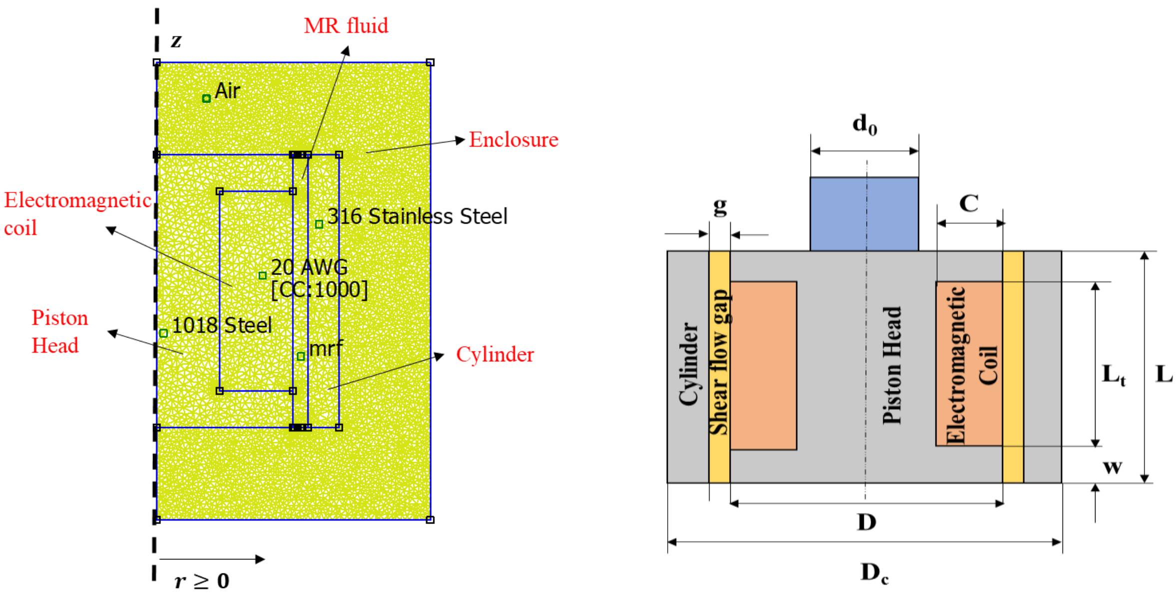


(a) (b)

Figure 3. (a) Grid structure model and (b) Components of MR damper

The 316-stainless steel has least magnetic permeability, which prevents the magnetic flux moving out of the cylinder and low carbon SA-1018 steel has greater value of magnetic permeability and it helps to develop higher magnetic flux density (MFD). The dynamic behavior of the MR damper is highly affected by the amount of magnetic field developed across the exposed area (flow region) of the shown damper. Also, the MFD developed is highly affected with the value of current supplied to the electromagnetic coil. The electromagnetic coil wound inside the piston head ($A$ = coil area in m$^2$) consists of 20 AWG copper wire wound with 1000 turns of coil ($N_c$ = number of turns in the coil). The number of turns has been kept constant for all sets of analysis. The MFD developed in the exposed area is calculated for the current in the range of 0 A to 5 A ($I$ = DC current). When the DC current is supplied to the electromagnetic coil a current density is occurred which is calculated with help of using Kirchoff's law as,

$$J = \frac{N_c I}{A} \tag{1}$$

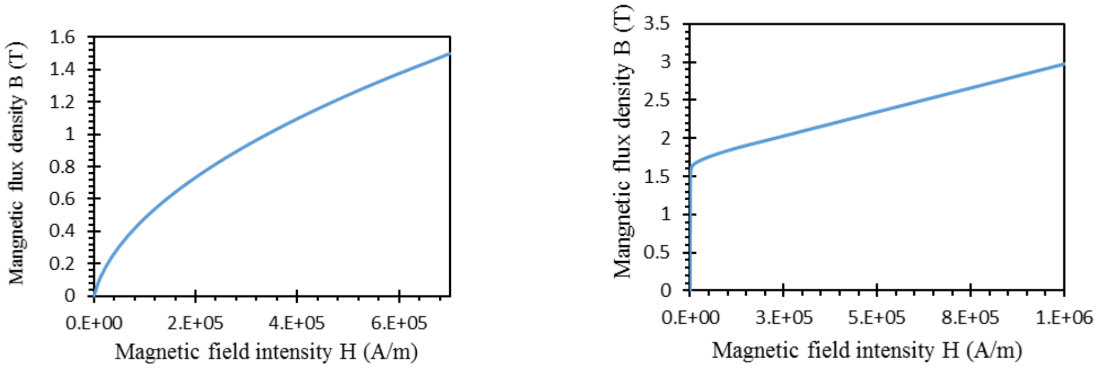


(a) (b)

Figure 4. MFD and MF Intensity plots of: (a) MR Fluid-132DG and (b) Low carbon-SA1018

Table 2. MR damper geometrical specifications

| Srl.No | Features | Values in mm |
|---|---|---|
| i | Outer radius of tube (Cylinder) ($D_c$/2) | 20 |
| ii | Piston rod diameter ($d_0$) | 10 |
| iii | Piston Radius (D/2) | 15 |
| iv | Length of channel (L) | 30 |
| v | Effective length ($L_t$) | 22 |
| vi | Thickens of web (w) | 2 |
| vii | Core depth (C) | 8 |
| viii | Annular Gap (g) | 1.5 |

## 4.0 RESULTS AND DISCUSSION

### 4.1 Magnetostatic Analysis Results

Figure 5(a) and (b) show the induced magnetic flux across the flow gap and whole body of the given damper. The values MFD increase with an increment in the value of electric current in DC provided to the electromagnetic coil. The MFD at the annular gap is computed for different currents in the range of 0.1 A to 5 A. The maximum magnetic flux obtained for 5 A of DC current is approximately 1.45 T as demonstrated in Figure 5(c). It can be clearly observed from Figure 5(d) that the enhancement of magnitude of MFD is significantly higher up to 3 A of current and it tends to decay after this limit. This behavior suggests that the electromagnetic coil shows a magnetic saturation beyond 3 A of current.

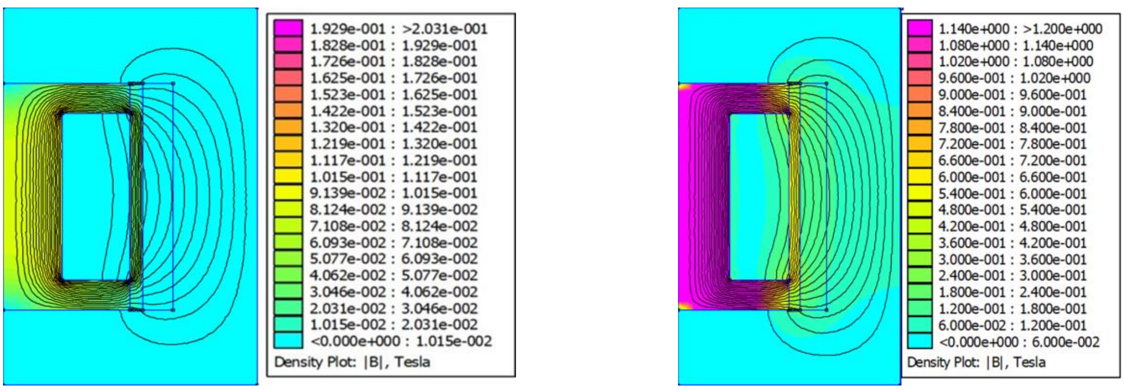


(a) (b)

Figure 5. Distribution of MFD at flow region for: (a) 0.1 A, (b) 5.0 A,

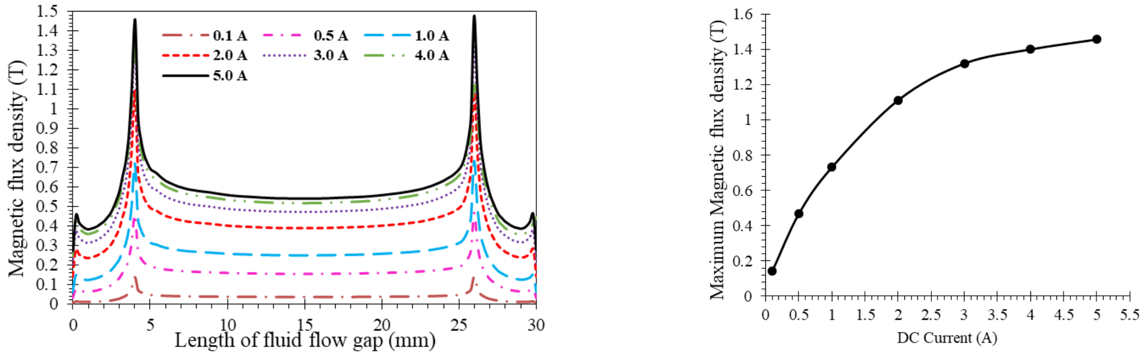


(c) (d)

Figure 5. (cont.) (c) variation of MFD and (d) magnetic saturation

## 4.2 Magneto Hydrodynamics of Fluid Flow

Here valve mode type MR damper model and only effective fluid flow region of damper are considered for the analysis. The fluid flowing through the gap is subjected to the external stimuli such as magnetic field in vertical to the fluid flow direction. Due to application of magnetic field, the carbonyl iron particles in the carrier silicon oil get magnetized and form chain like structure in the direction of the field (polarization) and results in development of yield shear stress. The gap has two regions, one is the region exposed to the magnetic field and another is under zero MFD. The magnetic field is applied over length from 2 mm to 28 mm, which is the length of the core coil where the magnetization of fluid occurs. The magnetic flux density which needs to be applied is obtained from the Magnetostatic FEA analysis. The governing equations are solved numerically under boundary conditions and initial set up by modeling in Fluent MHD. The equations which allow pairing between the magnetic property and rheological property are evaluated from Maxwell's and Ohms laws. Electromagnetic fields are described by Maxwell's equations (Dumitru[23]).

From Gauss law of magnetization,

$$\Delta \cdot B = 0 \tag{2}$$

From Gauss law,

$$\Delta \cdot E = \frac{q}{\varepsilon} \tag{3}$$

From Faraday Induction Law,

$$\Delta \cdot E = \frac{\partial B}{\partial t} \tag{4}$$

Current density according to Ohm's Law,

$$J = \sigma E \tag{5}$$

Under the influence of magnetic force '*B*' the velocity, *V* of the fluid is taking the form,

$$J = \sigma[E + V \times B] \tag{6}$$

Governing equation of steady flow between two parallel plates is (Gedik et al. [6]),

$$\Delta \cdot V = 0 \tag{7}$$

$$\rho\left(\frac{\partial V}{\partial t} + (V \cdot \nabla)V\right) = -\nabla P + \eta \Delta V + [J \times B] \tag{8}$$

where, $q$ is the charge density, $\varepsilon$ is electric permittivity (F/m), $\sigma$ is the electrical conductivity, $E$ is the electrical field intensity vector (V/m), $V$ is velocity (m/s), $P$ is the pressure gradient (Pa), $D$ is the electric induction field (C/m$^2$), $J$ is the current density (C/m$^3$), $\eta$ is dynamic viscosity, $B$ is the magnetic flux density (T), and $\rho$ is the density.

While conducting the CFD simulation, in order to reduce the computational efforts, the annular gap is modelled as the axisymmetric taking only the 45$^0$ sections of the entire domain as shown in Figure 6. The flow is considered as laminar, steady state and incompressible and the boundary conditions specified are, (i) pressure inlet (ii) pressure outlet (iii) no slip wall condition at inner and outer wall (iv) magnetic field perpendicular to the fluid flow for length of 28 mm and (v) symmetry condition. There are totally 95 040 hexahedral elements and 112700 nodes with mesh size of 0.025 mm, generated in the ANSYS fluent commercial code. The properties of MR fluid taken in this work are presented in Table 3.

The analysis was conducted at constant pressure gradient throughout the simulation. The pressure inlet conditions specified at the top surface of the cylinder are 25 kPa, 50 kPa and 75 kPa.

Table 3. MR fluid 132-DG -parameters and values (Lord co.)[24]

| Property | Value |
|---|---|
| Apparent Viscosity | 0.112 ± 0.02 Pa |
| Permeability (Magnetic) | 0.7, 0.5, 0.33 and 0.25 s |
| Density of the fluid | 2.95-3.15 g/cm3 |
| Range (Temp) | -40 to +130 °C |
| Specific Heat | 800 (J/kg K) |

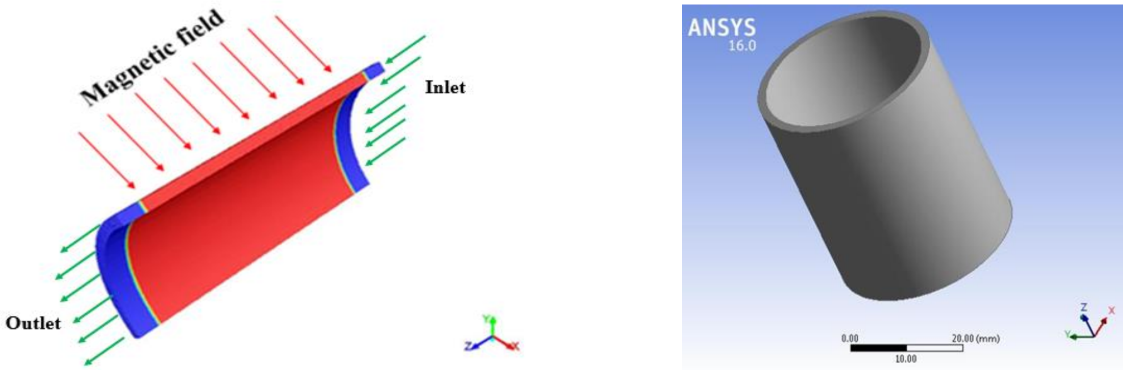


Figure 6. 3D model of annular channel and the axisymmetric 450 slices of the computational domain

The mesh sensitivity analysis was carried out to find the optimal element size for the analysis. Table 4 shows the mesh sensitivity check data and it can be observed that the percentage change in the velocity at the annular gap for fine mesh size is significantly less when compared to other mesh sizes. Hence, for present analysis fine mesh has been chosen.

Table 4. Mesh sensitivity check

| Sr.No | Size of Grid | No. of Grids | Average Fluid velocity (m/s$^2$) | Variation (%) |
|---|---|---|---|---|
| i | Coarse | 12 000 | 0.7496 | - |
| ii | Medium | 22 100 | 0.7234 | 3.5 |
| iii | Fine | 1 10 300 | 0.711 | 1.7 |

### 4.3 MHD Simulation Results

The influence of external magnetic field on the fluid flow through the annular gap of MR damper was investigated by considering flow mode. The change in the flow velocity was evaluated at different magnetic field values computed from the FE analysis. The length of the effective region in the annular gap was 28 mm which was exposed to the magnetic field leading to change of rheological properties of MR fluid. These changes further affect the flow behavior, which is as similar as non-Newtonian flow. Figure 7 depicts the velocity contour of MR fluid across the annular fluid flow gap. It can be observed that the velocity tends to decrease as the magnetic flux density increases. The reduction is evident at the effective area of the annular gap where the fluid is exposed to the magnetic field. Ferrous particles in the fluid form a chain like structure and fluid becomes viscoelastic in nature and behaves as non-Newtonian. These chains offer a resistance to fluid flow. Flow can only occur when the pressure applied exceeds the interparticle forces leading to breaking the bond between the particles (yazid et al.[25]). Figure 8 illustrates the velocity profile across the sections positioned near to the Inlet, Outlet and effective area of the flow region for 50 kPa pressure. It can be observed from figures that the velocity tends to decrease upon increment of magnetic field. Variations in the velocity are significant at the effective area (middle) when compared to the changes at inlet and outlet areas. The maximum velocity at the mid-section of effective area is 0.7682 m/s for 0.25 T of magnetic flux and velocity for 1 T is 0.56 m/s. Percentage reduction of velocity at the effective area (middle) is 17 %, while inlet and outlet regions have 11 % and 8 % respectively. Figure 9 shows the variation in velocity of the fluid due to the magnetic field for the inlet pressure of 25 kPa. From the figure, it can be seen that upon increasing the magnetic flux density from 0.25 T to 1 T, the reduction in the velocity at inlet, outlet and middle portion are 11.29 %, 5.68 % and 15.52 % respectively. It is clear that the maximum resistance to the fluid flow occurs at the region where the magnetic field is highly concentrated. The variation in the velocity of the fluid which is subjected to 75 kPa pressure and magnetic field from 0.25 T to 1 T is as shown in the Figure 10.

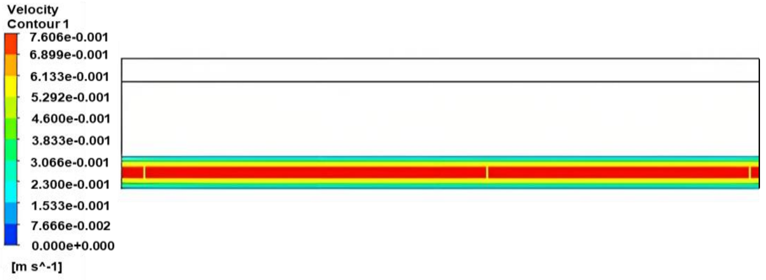


(a)

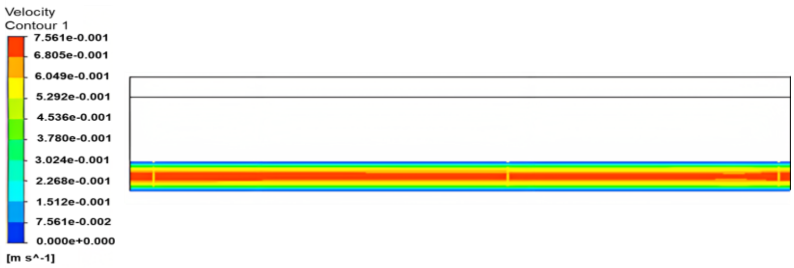


(b)

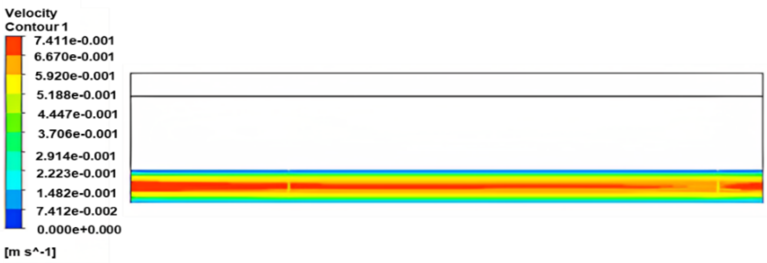


(c)

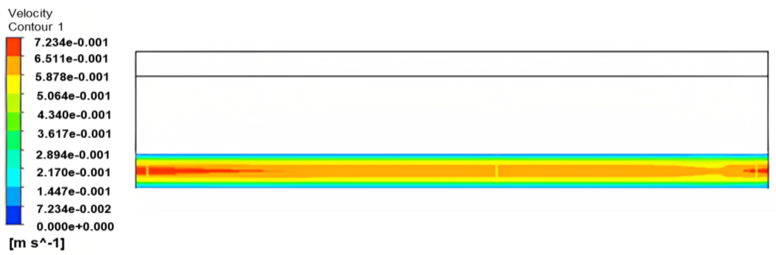


(d)

Figure 7. Velocity contours at annular gap under different magnetic fields: (a) 0.25 T, (b) 0.5 T, (c) 0.75 T and (d) 1.0 T

It can be seen that upon increasing the magnetic flux density from 0.25 T to 1 T, the reduction in the velocity at inlet, outlet and middle portion are 3.77 %, 6.07 % and 10.42 % respectively. On comparing the reduction of the velocity for different input pressures it was observed that maximum reduction occurred at lower pressure when compared to the higher pressure. The maximum velocity of fluid at 25 kPa pressure is 0.364 m/s, at 50 kPa pressure is 0.75 m/s and at 75 kPa pressure is 0.858 m/s. The percentage reduction is 16.52 % at 25 kPa, 14.86 % at 50 kPa and 10.42 % at 75 kPa pressure. Hence it is clearly evident that maximum reduction has occurred at lower pressure when compared to the higher-pressure inputs.

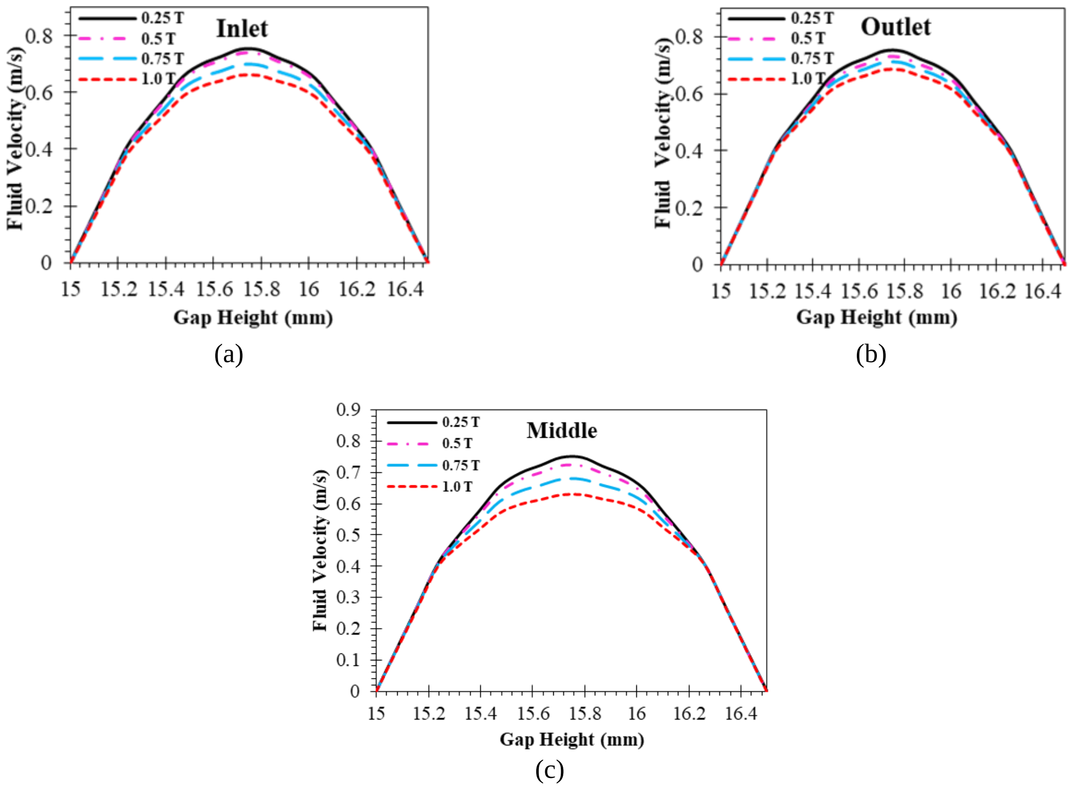


Figure 8. Velocity profiles for 50 kPa pressure at: (a) outlet, (b) inlet and (c) middle location of the flow gap for different currents

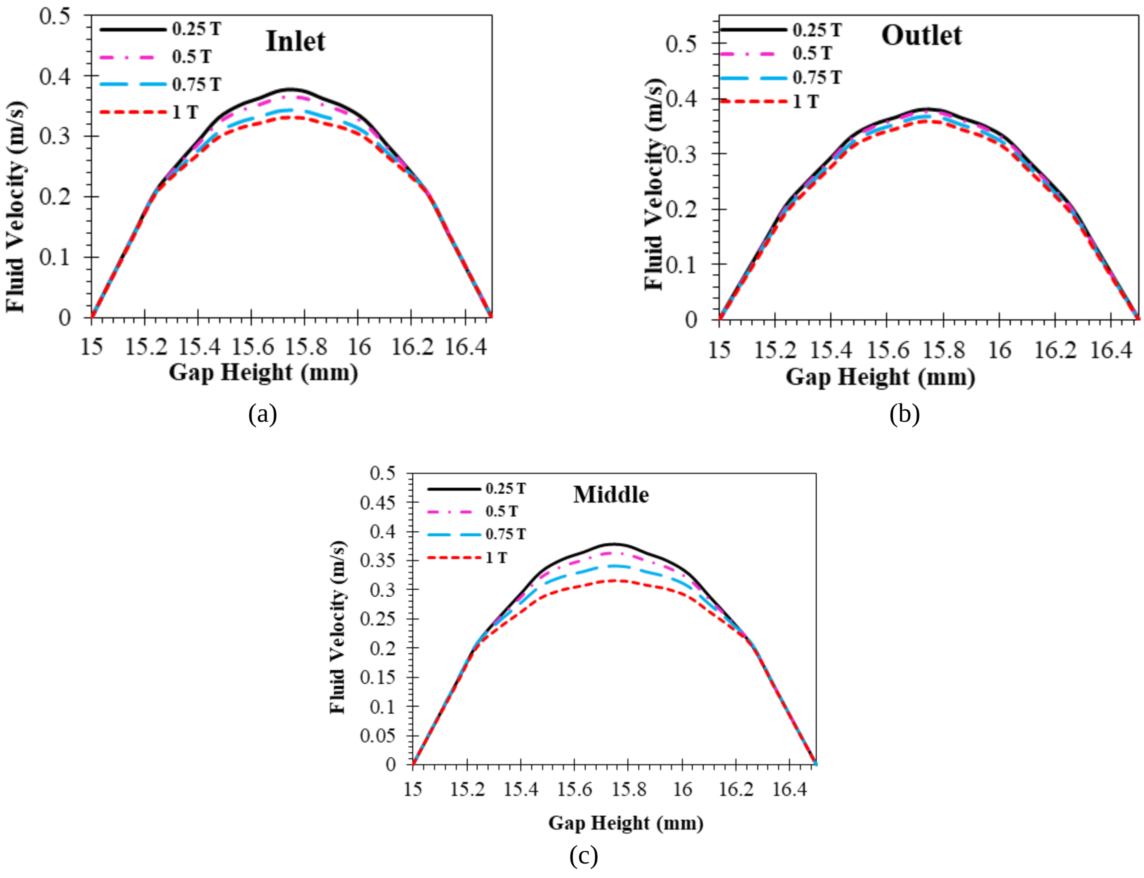


Figure 9. Velocity profiles for 25 kPa pressure at: (a) outlet, (b) inlet and (c) middle location of the flow gap for different currents

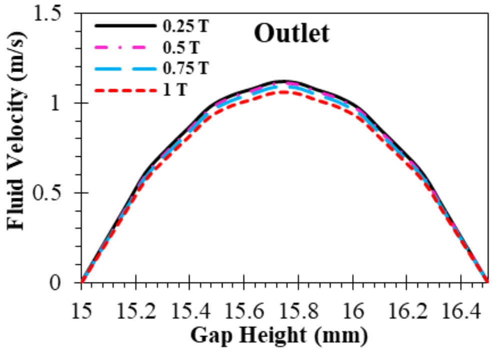


(a)

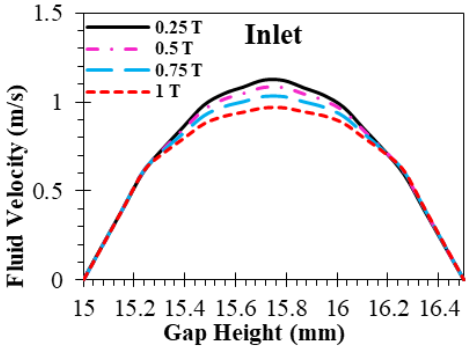


(b)

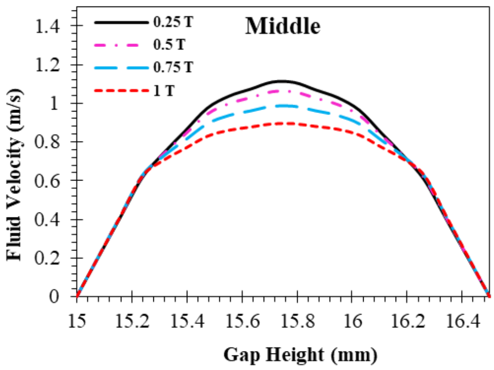


(c)

Figure 10. Velocity profiles for 75 kPa pressure at: (a) outlet, (b) inlet and (c) middle location of the flow gap for different currents

## 5.0 CONCLUSIONS

In this study, flow performance of MR fluid under the impact of external magnetic force was investigated through finite element analysis followed by CFD magnetohydrodynamic analysis in ANSYS FLUENT MHD module. The magnetic flux density was computed through FE analysis and was applied normal to the direction of flow of MR fluid at constant pressure gradient. The reduction in the velocity for different magnetic fields was evaluated at three locations of flow regime, i.e at inlet, outlet and effective area (middle section where the magnetic field applied). The results obtained from the analysis revealed that a significant reduction in the fluid flow was seen at the effective area of the annular gap. The maximum reduction in the velocity is found to be 15 % at middle position of the flow channel. On comparing the reduction of the velocity for different input pressures it was observed that maximum reduction occurred at lower pressure when compared to the higher pressure. The reduction of velocity indicates the resistance offered due to the variation of rheological properties of magnetically excited MR fluid. This resistance plays a vital role in enhancement of damping characteristic of an MR damper.

## 6.0 REFERENCES

[1] J. Rabinow, "The magnetic fluid clutch," *Electrical Engineering*, vol. 67, no. 12, pp. 1167-1167, 1948.

[2] J. D. Carlson, "Low-cost MR fluid sponge devices," *Journal of Intelligent Material Systems and Structures*, vol. 10, no. 8, pp. 589-594, 1999.

[3] G. TharehalliMata, H. Krishna, and M. Keshav, "Characterization of magneto-rheological fluid having elongated ferrous particles and its implementation in MR damper for three-wheeler passenger vehicle," *Proceedings of the Institution of Mechanical Engineers, Part D: Journal of Automobile Engineering*, vol. 237, no. 2-3, pp. 426-439, 2023.

[4] J. Wang, G. Meng, "Magnetorheological fluid devices: Principles, characteristics and applications in mechanical engineering," *Proceedings of the Institution of Mechanical Engineers, Part L: Journal of Materials: Design and Applications*, vol. 215, no. 3, pp. 165-174, 2001.

[5] N. Wereley, "Magnetorheology: Advances and applications," 6th Edition, *Royal Society of Chemistry*, 2013.

[6] E. Gedik, H. Kurt, and Z. Recebli, "CFD simulation of Magnetohydrodynamic flow of a liquid-metal Galinstan fluid in circular pipes," *Fluid Dynamics and Materials Processing*, vol. 9, pp. 23-33, 2013.

[7] D. A. Case, B. Taheri, and E. Richer, "Multiphysics modelling of magnetorheological dampers," *The International Journal of Multiphysics*, vol. 7, no. 1, pp. 61–76, 2013.

[8] A. Sternberg, R. Zemp, and J. C. de la Llera, "Multiphysics behaviour of a magnetorheological damper and experimental validation," *Engineering Structures*, vol. 69, pp. 194–205, 2014.

[9] E. J. Park., Luis Falcao da Luz, and S. Afzal, "Multidisciplinary design optimization of an automotive magnetorheological brake design," *Computers and Structures*, vol. 86, no. 3, pp. 207-216, 2008.

[10] T. M. Gurubasavaraju, "Estimation of damping force of double ended Magnetorheological damper through one way coupled CFD and FEA analysis," *Journal of The Institution of Engineers (India): Series C*, vol. 102, no. 5, pp. 1145-1151, 2021.

[11] F. Zschunke, P. O. Brunn, and M. Steven, "Simulation of a magnetorheological damper with a combination of a commercial CFD and FEA code," *ASME Pressure Vessels and Piping Conference,* vol. 3097, pp. 119-124, 2004.

[12] E. Gedik, H. Kurt., Z. Recebli, and C. Balan, "Two dimensional CFD simulation of magnetorheological fluid between two fixed parallel plates applied external magnetic field," *Computers and Fluids*, vol. 63, pp. 128-134, 2014.

[13] F. Omidbeygi, and S. H. Hashemabadi, "Exact solution and CFD simulation of magnetorheological fluid purely tangential flow within an eccentric annulus," *International Journal of Mechanical Sciences*, vol. 75, pp. 26-33, 2013.

[14] M. Diudea, V. Hodor, R. Bălan, and M. Bara, "CFD prediction of the flow inside the damper by the use of LES model," *Bulletin of the Transilvania University of Brasov, Engineering Sciences Series I*, vol. 6, no. 2, pp. 1-7, 2013.

[15] G. Tharehallimata, K. L. Narasimhamu, "Geometric optimisation of double ended magnetorheological fluid damper," *International Journal on Interactive Design and Manufacturing,* vol. 17, pp. 1339–1349, 2023.

[16] J. Zheng, Z. Li, J. Koo and J. Wang, "Magnetic circuit design and multiphysics analysis of a novel MR damper for applications under high velocity," *Advances in Mechanical Engineering*, vol. 9, pp. 1–16, 2014.

[17] Q. H. Nguyen, Y. M. Han, S. B. Choi, and N. M. Wereley, "Geometry optimization of MR valves constrained in a specific volume using the finite element method," *Smart Materials and Structures*, vol. 16, no. 6, pp. 2242–2252, 2007.

[18] J. Goldasz, and B. Sapinski, "Verification of magnetorheological shock absorber models with various piston configurations," *Journal of Intelligent Material Systems and Structures,* vol. 24, no. 15, pp. 1846-1864, 2013.

[19] T. M. Gurubasavaraju, H. Kumar and A. Mahalingam, "An approach for characterizing twin-tube shear-mode magnetorheological damper through coupled FE and CFD analysis," *Journal of the Brazilian Society of Mechanical Sciences and Engineering*, vol. 40, no. 3, pp. 139, 2018.

[20] M. M. Ferdaus, M. M. Rashid, M. H. Hasan and M. A. Rahman, "Optimal design of Magneto-Rheological damper comparing different configurations by finite element analysis," *Journal of Mechanical Science and Technology*, vol. 28, no. 9, pp. 3667-3677, 2014.

[21] S. H. Tu and W. S. Jeng, "Finite element analysis of a magnetorheological fluid damper," *CSME Conference*, Taiwan, 2007.

[22] D. Wang., B. Zi., S. Qian., and J. Qian, "Steady-state heat-flow coupling field of a high-power magnetorheological fluid clutch utilizing liquid cooling," *Journal of Fluids Engineering,* vol. 139, no. 11, p. 111105, 2017.

[23] C. A. Dumitru, "Numerical problems in 3D magnetostatic FEM analysis," *Advances in Automatic Control, Modelling & Simulation, Recent Advances in Electrical Engineering Series*, vol. 13, pp. 385-390, 2013.

[24] Lord Corporation, "MRF-132DG Magneto-rheological fluid," Technical Data, 2008. [Online]. Available: https://lordfulfillment.com/pdf/44/DS7015_MRF-132DGMRFluid.pdf.

[25] I. I. Mohd Yazid, S. A. Mazlan, T. Kikuchi T, H. Zamzuri and F. Imaduddin, "Design of magnetorheological damper with a combination of shear and squeeze modes," *Materials & Design*, vol. 54, pp. 87-95, 2014.